Sheared Boundary Layers in Turbulent Rayleigh-Bénard Convection

T. H. Solomon and J. P. Gollub
Department of Physics, Haverford College, Haverford, Pennsylvania 19041
and Department of Physics, University of Pennsylvania, Philadelphia, Pennsylvania 19104
(Received 2 February 1990)

Thermal boundary layers in turbulent Rayleigh-Bénard convection are studied experimentally using a novel system in which the convecting fluid is sheared from below with a flowing layer of mercury. Oscillatory shear substantially alters the spatial structure and frequency of the eruptions, with minimal effect on the heat flux ($< 5\%$). The temperature probability distribution function (PDF) just above the lower boundary layer changes from Gaussian to exponential, without significant changes in the interior PDF. Implications for theories of "hard" turbulence are discussed.

PACS numbers: 47.25.Qv, 47.20.Bp, 47.25.Ae, 92.60.Fm

The role of thermal or viscous boundary layers in turbulent flows is a problem of fundamental interest. Intermittent bursts from boundary layers produce coherent structures that propagate through the bulk, determining the statistical properties of the flow.[1] In addition, the transport of heat and momentum across the system is often limited by the boundary layers (BL's). For these reasons, much can be learned about turbulent flows by studying their properties. This is especially true for turbulent Rayleigh-Bénard (RB) convection, in which the temperature gradient is concentrated in thin, stagnant (but unstable) thermal BL's near the upper and lower surfaces.[2] This system has attracted much attention recently because of the discovery[3] of scaling laws in the heat flux and temperature statistics over many orders of magnitude of the Rayleigh number R (the dimensionless temperature difference across the fluid). Motions arising from boundary-layer eruptions are also important in understanding convection in the atmosphere and oceans.[4]

Most theories of heat transport in turbulent RB convection assume marginal stability of the thermal BL's, which grow in thickness to an average value δ where they become unstable to thermal eruptions. Early investigators[2] proposed that, for large R, δ is independent of the height of the convection cell and properties of the interior flow. The temperature gradient was assumed concentrated entirely in the BL's, and as a result the Nusselt number Nu (the nondimensional heat flux) should grow as R^{β}, with $\beta = \frac{1}{3}$. Experiments[5] have found that $\beta \cong \frac{2}{7}$ at large R, prompting the hypothesis[3,6] that shearing "winds" from the interior increase δ, lowering Nu. In addition, instabilities of the BL's to wavelike propagation of thermal disturbances were also suggested[7] to explain the observed transition from "soft" to "hard" turbulence, a transition characterized by a change in the temperature probability distribution function (PDF) at the center of the cell from Gaussian to exponential.[3]

In this Letter, we describe experimental studies of BL dynamics using a novel approach in which the convecting fluid is sheared from below with a layer of mercury that acts as a constant-temperature, moving boundary. The behavior of the lower BL is controlled primarily by interactions with this "artificial wind" from below. Measurements of Nu and of the spacing and frequency of the BL eruptions when sheared externally are contrasted with those for the normal (unsheared) case. The effects of the shear on the temperature PDF's in the interior are also examined.

A diagram of the convection apparatus is shown in Fig. 1, along with a sketch of the driving mechanism for the mercury flow. The convecting fluid is water at temperatures between 30 and 40°C (Prandtl number Pr $\cong 25$) in enclosures of horizontal size 6.35×6.35 cm^2, and depths 4.0 and 9.0 cm. For these experiments, R is varied between 10^6 and 10^8. A layer of mercury 7 mm deep forms the bottom of the convection cell. Local measurements of the temperatures at two locations in the fluid are made with small thermister probes 0.5 mm in diameter. One probe is located 2 to 3 mm above the mercury-water interface, centered laterally, and the other is located at the midheight of the cell. A thin, laminated copper plate with a resistive heater separates the mercury from a configuration of permanent magnets (neodymium iron boron). Measurements of the heat flux are determined from the power required to keep the mercury at a constant temperature. The heater and magnets are surrounded from below by insulation and an aluminum block that is separately controlled at the temperature of the mercury to prevent heat leakage. In addition, the sides of the cell are well insulated.

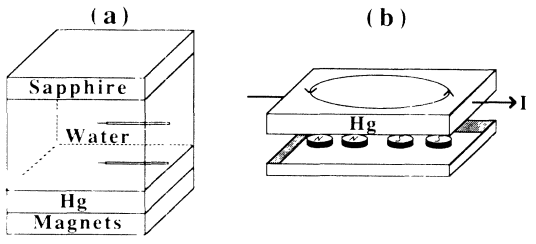

FIG. 1. (a) A schematic diagram of convection apparatus, showing temperature probes in the water layer. The sapphire window and mercury are maintained at constant temperatures. (b) Exploded view of magnetohydrodynamic forcing of a vortical flow in the mercury layer.

A flow is induced in the mercury using a magnetohydrodynamic technique[8] [Fig. 1(b)] in order to shear the lower BL. A uniform electrical current passing horizontally through the mercury interacts with an alternating vertical magnetic field imposed by magnets located below the mercury. These interactions produce vortex flows in the mercury with velocities that are continuously varied by changing the current, and spatial structures that can be altered by changing the magnet configuration. Except where otherwise stated, the shearing flow is a single vortex whose characteristic speed (rms) is in the range 0–6 mm/s. These velocities should be compared to the typical rms horizontal convective velocities just above the lower BL, which range up to approximately 0.8 mm/s at $R \approx 10^8$. The mercury flow is made to oscillate by employing a bipolar, square-wave current with frequency 0.20 Hz that is chosen to confine the shear to the vicinity of the BL. (This is necessary to distinguish the effects of shear on the BL from those on the interior flow.) At this frequency, the imposed shear has a characteristic thickness of 1.9 mm, close to the typical BL thickness δ (2.1 mm at $R = 5.7 \times 10^7$, for example). Secondary flows due to unbalanced centrifugal forces near the boundary are negligible with this forcing configuration, so the induced flows in the convecting fluid are predominantly horizontal.

Bursting of the BL is studied with a technique that allows direct visualization of the temperature field. Thermochromic liquid-crystal (TLC) microspheres are suspended in the convecting fluid.[9] A thin, vertical section of the fluid is illuminated with a sheet of white light, and the resulting scattered light is imaged from the side. The color and intensity of the scattered light vary with the temperature of the fluid. In addition, observations of the movements of the microspheres provide information about the velocity field. A color video camera allows the bursting of the lower thermal boundary layer and the resulting interior temperature distribution to be analyzed. An example of a TLC image is shown in Fig. 2.

Sequences of enhanced TLC images of eruptions of the lower BL are shown in Fig. 3. In the unsheared case [Fig. 3(a)], recirculation zones form at the base of each developing burst, pulling hot fluid laterally from surrounding areas of the BL and increasing the heat content of the plume. These recirculation zones also cause separate plumes to aggregate, as can be seen in Fig. 3(a). The resulting eruptions have lateral dimensions up to 4 times larger than the thickness of the BL.

In the sheared case [Fig. 3(b)], the movement of hot fluid in and near the BL is determined primarily by the external forcing and is less influenced by recirculation. Regions of hot fluid remain isolated and burst separately, rather than aggregating. As a result, the eruptions are more frequent, but the resulting thermals are small (comparable to the boundary-layer thickness), and their heat content is less. This behavior is reflected in power spectra of temperature fluctuations measured by the lower probe. The average fluctuation frequency (charac-

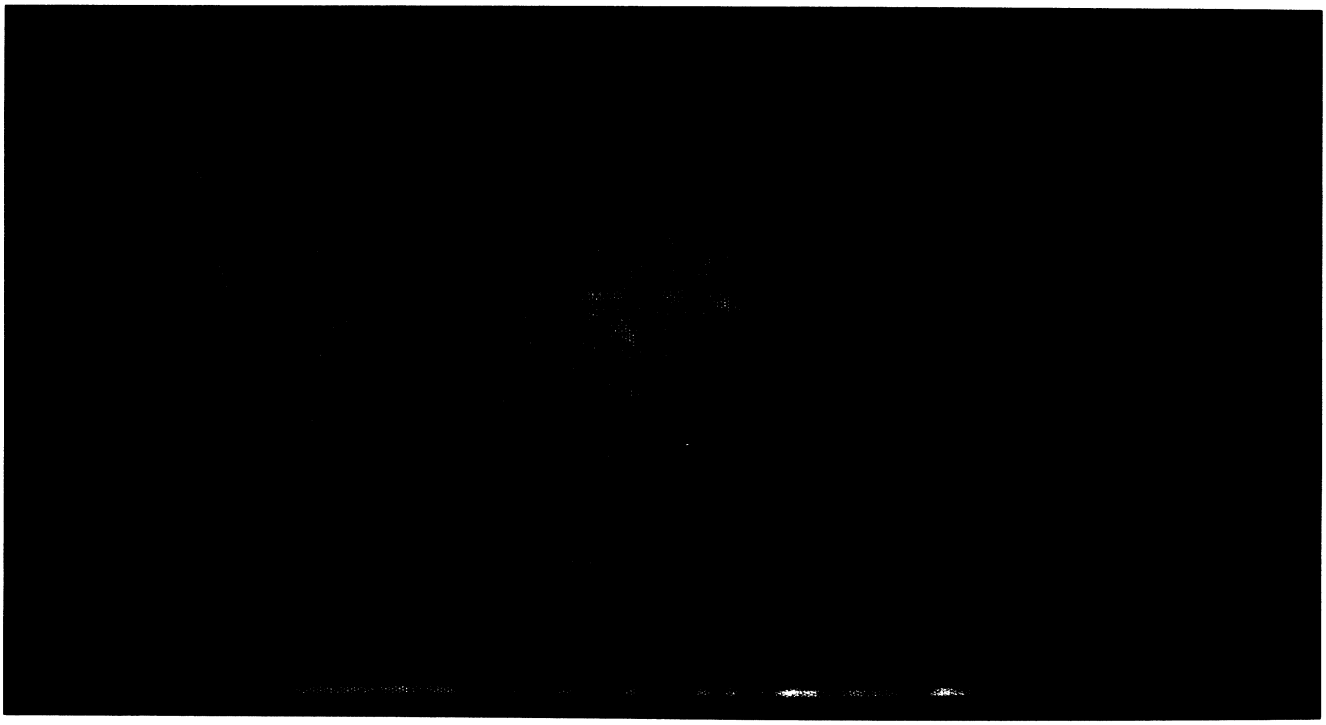

FIG. 2. Thermochromic liquid-crystal imaging of a vertical section of the convection cell (except for the top $\frac{1}{4}$ in.) at $R = 8.1 \times 10^6$, $d = 4.0$ cm. The lower boundary layer and warm eruptions are blue; red-brown regions are cooler.

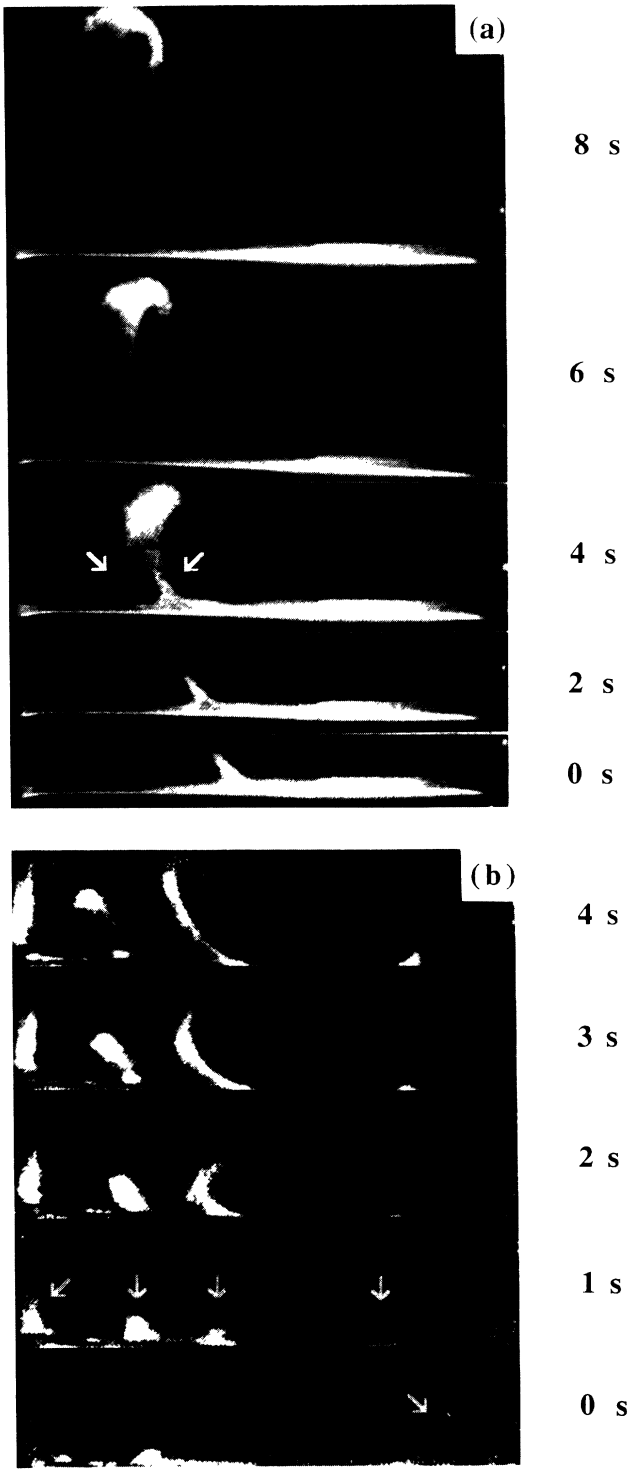

FIG. 3. Eruptions of the lower boundary layer for $R = 1.1 \times 10^8$ and $d = 9.0$ cm. In these images, the light regions (actually blue) correspond to warm fluid. The full width of the cell is shown (but not the full height). (a) Unsheared convection: Two hot sections of the boundary layer aggregate while erupting (see arrows). (b) Convection sheared by an oscillating mercury flow of rms velocity 6 mm/s. Sections of the boundary layer erupt separately, increasing the frequency of bursting.

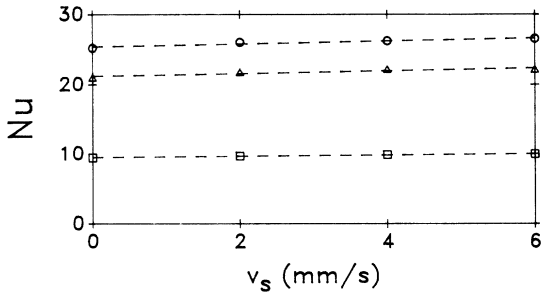

FIG. 4. Dependence of heat flux on rms forcing velocity v_s: $R = 4.6 \times 10^6$ (□), 5.7×10^7 (△), 1.1×10^8 (○).

terized by the first moment of the power spectrum) increases monotonically by a factor of 3–4 over the range of forcing velocities studied. It is clear from these observations that external (and internal) shearing winds influence the organization of thermal eruptions from the BL. However, their effect on the heat flux is surprisingly small (Fig. 4). The Nusselt number increases by up to 5% in the presence of oscillating shear flows, independent of R.

Measurements of temperature PDF's in the *unsheared* convective flow are presented in Figs. 5(a) and 5(b). The scaled PDF's just above the lower BL [Fig. 5(a)] are approximately Gaussian and are independent of R over the range studied, as indicated by the different symbols. The PDF's in the center of the cell [Fig. 5(b)], on the other hand, depend on R. They are exponential for $R \gtrsim 3 \times 10^7$, the regime of hard turbulence. Below $R \approx 10^7$, the center PDF's are mixed, having exponential peaks but Gaussian tails. This change in the behavior of

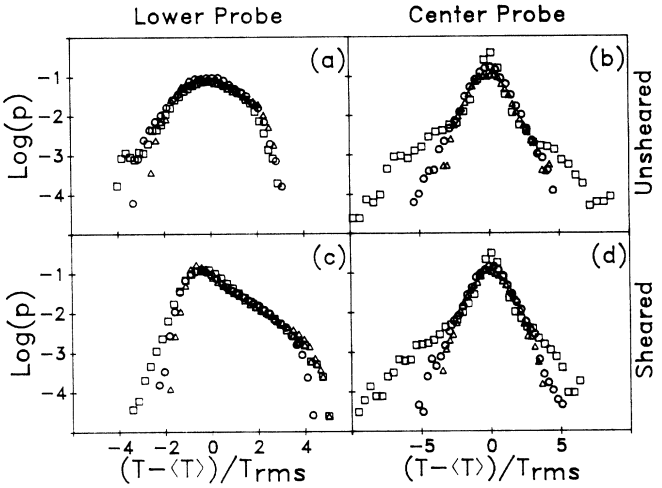

FIG. 5. Temperature probability distribution functions: $R = 4.9 \times 10^6$ (□), 5.7×10^7 (△), 1.1×10^8 (○). The data are scaled by subtracting the mean temperature $\langle T \rangle$ and dividing by the rms temperature fluctuations T_{rms}. (a) Unsheared, lower probe; (b) unsheared, center probe; (c) sheared (6 mm/s), lower probe; (d) sheared, center probe.

the PDF's marks a transition between turbulent convective regimes, similar to the soft-to-hard transition observed in Ref. 3. However, these "soft-turbulence" PDF's are fundamentally different from those of Ref. 3 at comparable R, which do not have exponential peaks. Mixed PDF's have also been observed in numerical simulations of soft turbulence.[10] Experimental tests indicate that the PDF's for R below 10^7 are purely Gaussian when the aspect ratio is sufficiently small. (We discovered this fact by inserting Plexiglas spacers in our shallow cell to reduce its aspect ratio to that of the taller one, 0.7.)

If the lower BL is sheared externally, the PDF's at the lower probe change from Gaussian to exponential with asymmetrical tails [Fig. 5(c)]. These changes in the lower PDF's are probably due to external shear preventing the organization of large coherent plumes, as seen in Fig. 3. (Changes in PDF's of this nature have been predicted in a recent theory[11] that relates them to the correlations between temperature and vertical velocity.) It is interesting that these lower PDF's, like those in the unsheared case, are independent of R. Whereas the scaled PDF's at the lower probe change dramatically in response to the external forcing, those in the center remain constant [Fig. 5(d)], with the exception of a slight change in the positive-temperature tail for $R = 4.9 \times 10^6$. (There are small shifts to higher $\langle T \rangle$ in the *unscaled* PDF's, but the standard deviation of temperature fluctuations remains constant.)

In conclusion, we have observed that the heat flux is not substantially affected by major shear-induced changes in the boundary-layer dynamics, as manifested in local power spectra, temperature probability distribution functions, and visual observations of the temperature field. It should be emphasized, however, that the heat flux is robust only if the forcing winds are strictly horizontal and limited to the vicinity of the BL. Substantial increases in Nu (up to 70%) are observed if the BL is perturbed by much more energetic forcing that produces secondary flows with significant vertical components.[12] *Decreases* in Nu, on the other hand, are observed in previous experiments[13] and simulations[14] on thermally stratified plane Couette flow, where imposed linear shears are *not* confined to the BL and appear to disrupt large-scale thermal structures in the interior.

Our results appear to be inconsistent with the hypothesis that shear-induced stabilization of the BL's (i.e., horizontal interior winds increasing the thickness δ at which the BL erupts) is responsible for the value of β ($\cong \frac{2}{7}$) observed at large R. Perhaps vigorous winds at large R cause the interior temperature distribution not to be strictly isothermal, as in Refs. 13 and 14, thus reducing the heat flux. Alternatively, several authors have proposed recently that δ is governed not by marginal stability but by a balance between diffusive heat flux into and advective heat flux out of the BL.[15] It is possible to explain the observed scaling behavior in this manner.

The absence of change in the lower PDF at the soft-to-hard transition suggests that a global analysis of the convecting layer is necessary to understand the transition. Visual observations using TLC imaging show that in the soft-turbulence regime the thermal plumes frequently span the full height of the cell (see Fig. 2), whereas at higher R they are broken into smaller structures before traversing the cell. These observations, along with those of the sensitivity of the center PDF's to aspect ratio at lower R (but not to BL shear), suggest that changes in the organization and coherence of thermal structures in the interior are a dominant feature of the soft-to-hard transition. Quantitative studies of the full temperature field may lead to a deeper understanding of these issues and are in progress.

We are pleased to acknowledge useful discussions with J. Domaradzki, E. Moses, M. Parsley, B. Shraiman, V. Yakhot, and S. Zaleski. The assistance of T. Davis in the construction of the convection apparatus is gratefully acknowledged. This work was supported by the University Research Initiative program under Contract No. DARPA/ONR N00014-85-K-0759.

[1]See, e.g., E. Mollo-Christensen, Annu. Rev. Fluid Mech. **5**, 101 (1973); W. W. Willmarth, Adv. Appl. Mech. **15**, 159 (1975).

[2]W. V. R. Malkus, Proc. Roy. Soc. London A **225**, 185 (1954); C. H. B. Priestley, Aust. J. Phys. **7**, 176 (1954); L. N. Howard, in *Proceedings of the Eleventh International Congress of Applied Mechanics, Munich,* edited by H. Görtler (Springer-Verlag, Berlin, 1966), p. 1109.

[3]B. Castaing, G. Gunaratne, F. Heslot, L. Kadanoff, A. Libchaber, S. Thomae, X. Z. Wu, S. Zaleski, and G. Zanetti, J. Fluid Mech. **204**, 1 (1989).

[4]See, e.g., G. S. Young, Earth Sci. Rev. **25**, 179 (1988).

[5]F. Heslot, B. Castaing, and A. Libchaber, Phys. Rev. A **36**, 5870 (1987). See also T. Y. Chu and R. J. Goldstein, J. Fluid Mech. **60**, 141 (1973); D. C. Threlfall, J. Fluid Mech. **67**, 17 (1975).

[6]S. Zaleski (private communication).

[7]S. Gross, G. Zocchi, and A. Libchaber, C. R. Acad. Sci. **307**, 447 (1988).

[8]J. Sommeria, J. Fluid Mech. **170**, 139 (1986); P. Tabeling, B. Perrin, and S. Fauve, Europhys. Lett. **3**, 459 (1987).

[9]H. S. Rhee, J. R. Koseff, and R. L. Street, Exp. Fluids **2**, 57 (1984); D. Dabiri and M. Gharib, Bull. Am. Phys. Soc. **34**, 2337 (1989).

[10]S. Christie and J. A. Domaradzki, Bull. Am. Phys. Soc. **34**, 2338 (1989).

[11]Y. G. Sinai and V. Yahkot, Phys. Rev. Lett. **63**, 1962 (1989); V. Yahkot, Phys. Rev. Lett. **63**, 1965 (1989).

[12]T. H. Solomon and J. P. Gollub (to be published).

[13]A. P. Ingersoll, J. Fluid Mech. **25**, 209 (1966).

[14]J. A. Domaradzki and R. W. Metcalfe, J. Fluid Mech. **193**, 499 (1988).

[15]Z.-S. She, Phys. Fluids A **1**, 911 (1989); B. I. Shraiman and E. Siggia (to be published).

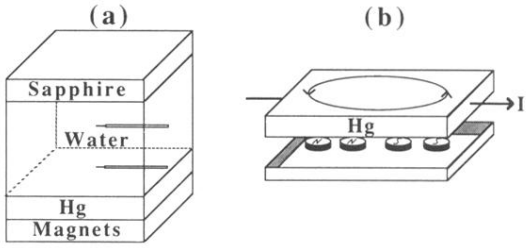

FIG. 1. (a) A schematic diagram of convection apparatus, showing temperature probes in the water layer. The sapphire window and mercury are maintained at constant temperatures. (b) Exploded view of magnetohydrodynamic forcing of a vortical flow in the mercury layer.

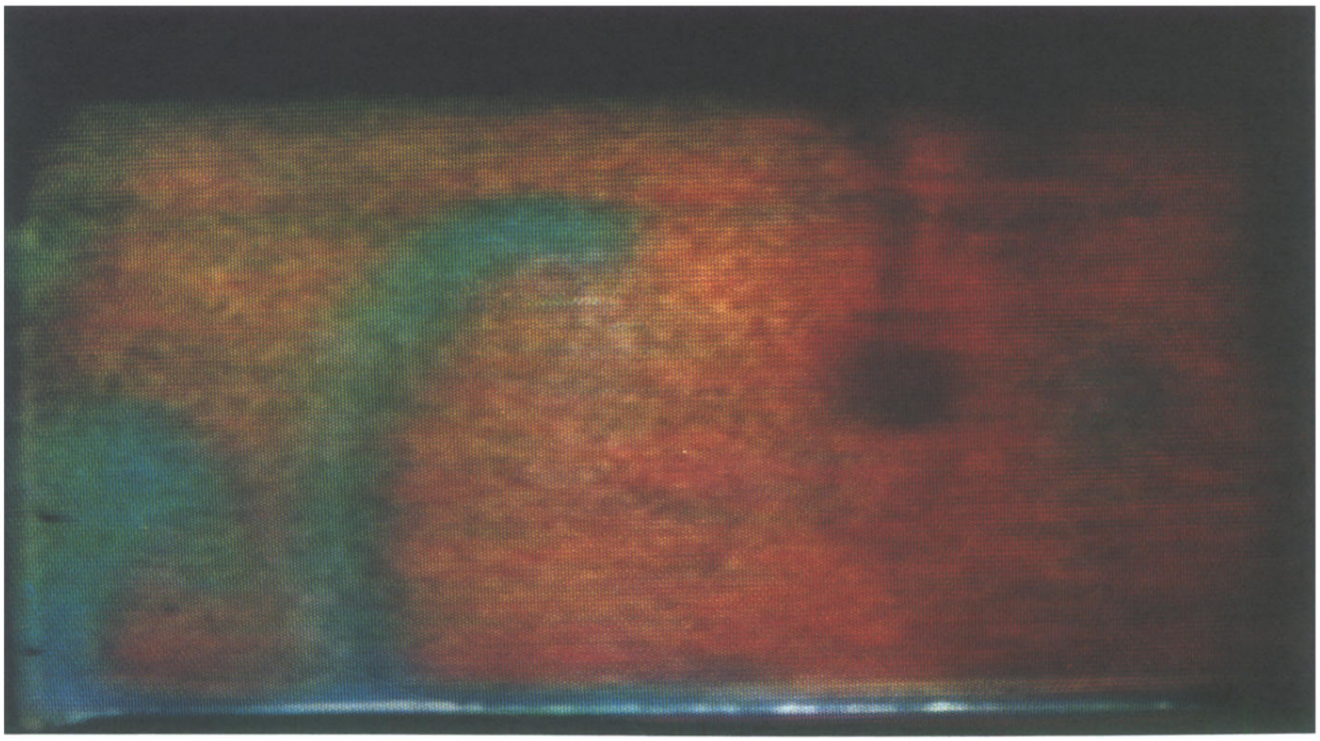

FIG. 2. Thermochromic liquid-crystal imaging of a vertical section of the convection cell (except for the top $\frac{1}{4}$ in.) at $R = 8.1 \times 10^6$, $d = 4.0$ cm. The lower boundary layer and warm eruptions are blue; red-brown regions are cooler.

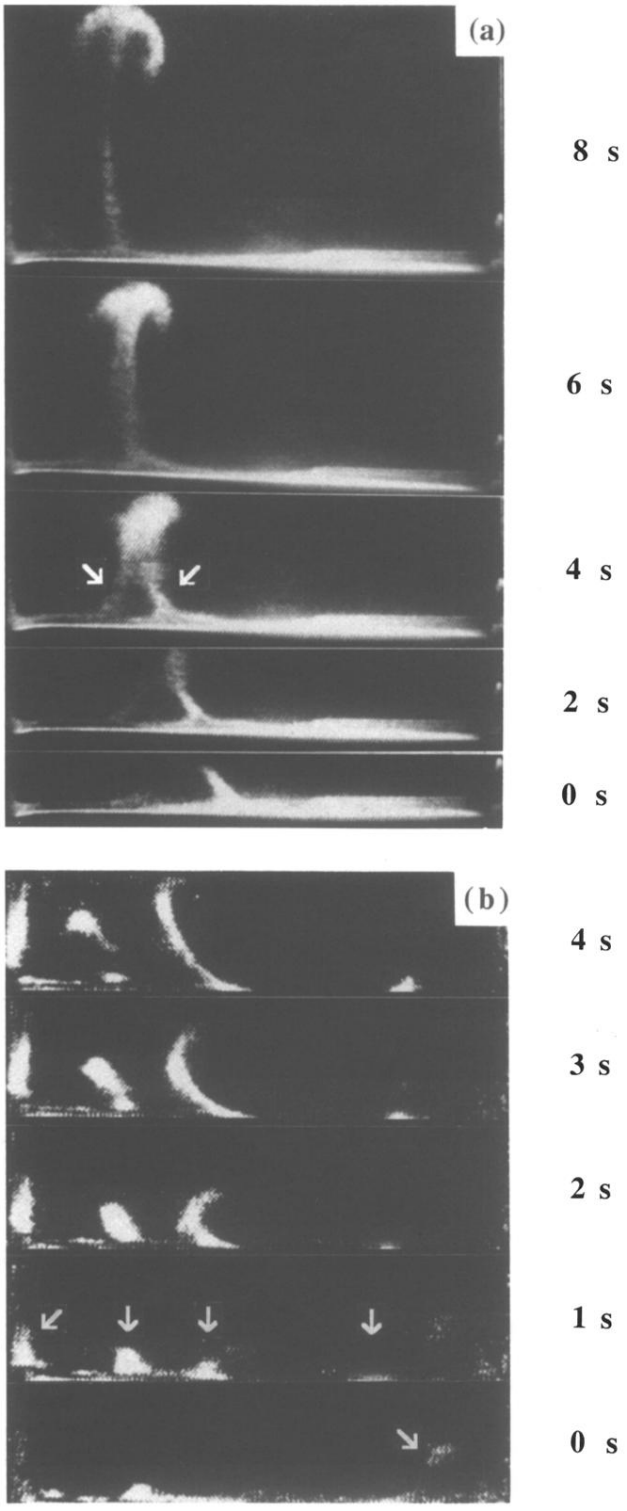

FIG. 3. Eruptions of the lower boundary layer for $R = 1.1 \times 10^8$ and $d = 9.0$ cm. In these images, the light regions (actually blue) correspond to warm fluid. The full width of the cell is shown (but not the full height). (a) Unsheared convection: Two hot sections of the boundary layer aggregate while erupting (see arrows). (b) Convection sheared by an oscillating mercury flow of rms velocity 6 mm/s. Sections of the boundary layer erupt separately, increasing the frequency of bursting.